BCAT-induced autophagy regulates Aβ load through an interdependence of redox state and PKC phosphorylation-implications in Alzheimer's disease. [†]

Harris, M.[‡*], El Hindy, M.[‡*], Usmari-Moraes, M.[‡*,] Hudd, F. [‡], Shafei, M. [‡] Dong, M. [¥],

Hezwani, M.[‡], Clark, P.[‡], House, M.[‡], Forshaw, T.[‡], Kehoe, P.[§], and Conway, ME[‡†]

[‡]Faculty of Health and Applied Sciences, University of the West of England, Coldharbor Lane, Bristol, BS16 1QY, UK.

[¥]Department of Chemistry, North Carolina Agricultural and Technical State University, Market Street, Greensboro, North Carolina, 27411, USA.

[§]Institute of Clinical Neurosciences, Learning and Research Building, Southmead Hospital, Bristol, United Kingdom.

*These authors contributed equally to the paper.

Running title: BCAT regulated autophagy and Aβ.

[*]Address correspondence: Myra E. Conway, Faculty of Health and Life Sciences, University of the West of England, Coldharbor Lane, Bristol, BS16 1QY, UK Tel: 0044 117 328 3552; Fax: 0044 117 328 2904; email: **myra.conway@uwe.ac.uk**.

ABSTRACT

Leucine, nutrient signal and substrate for the branched chain aminotransferase (BCAT) activates the mechanistic target of rapamycin (mTORC1) and regulates autophagic flux, mechanisms implicated in the pathogenesis of neurodegenerative conditions such as Alzheimer's disease (AD). BCAT is upregulated in AD, where a moonlighting role, imparted through its redox-active CXXC motif, has been suggested. Here we demonstrate that the redox state of BCAT signals differential phosphorylation by protein kinase C (PKC) regulating the trafficking of cellular pools of BCAT. We show inter-dependence of BCAT expression and proteins associated with the P13K/Akt/mTORC1 and autophagy signalling pathways. In response to insulin or an increase in ROS, BCATc is trafficked to the membrane and docks via palmitoylation, which is associated with BCATc-induced autophagy through PKC phosphorylation. In response to increased levels of BCATc, as observed in AD, amyloid β (Aβ) levels accumulate due to a shift in autophagic flux. This effect was diminished when incubated with leucine, indicating that dietary levels of amino acids show promise in regulating Aβ load. Together these findings show that increased BCATc expression, reported in human AD brain, will affect autophagy and Aβ load through the interdependence of its redox-regulated phosphorylation offering a novel target to address AD pathology.

KEYWORDS: BCAT, phosphorylation, redox regulated, PKC, insulin signalling, autophagy, Aβ.

Abbreviations:
α-ketoisocaproate (KIC), and α-ketoisovalerate (KIV), α-keto-β-methylvalerate (KMV) Alzheimer's disease (AD), amyloid β (Aβ), branched chain amino acids (BCAA), branched chain aminotransferase (BCAT), cytosolic BCAT (BCATc), mitochondrial BCAT (BCATm), branched chain α-keto acid dehydrogenase (BCKD), Glutamate dehydrogenase (GDH), glutathione (GSH), mechanistic target of rapamycin (mTORC1), hydroxylamine (HAM), leucine deprivation (LD), N-ethyl maleimide (NEM), , oxidised glutathione (GSSG), phorbal 12-myristate 13-acetate (PMA), protein kinase C (PKC), phenylmethanesulfonyl fluoride (PMSF), S-Nitrosoglutathione (GSNO), staurosporine (SS).

INTRODUCTION

The branched chain aminotransferase proteins (BCAT), BCATm (mitochondrial) and BCATc (cytosolic) catalyse the transamination of the branched chain amino acids (BCAA), leucine, valine and isoleucine to their respective α-keto acids and glutamate (Ichihara, 1975., reviewed in Conway and Hutson, 2016). Complete oxidation of the resulting α-keto acids, by the branched chain α-keto acid dehydrogenase complex (BCKDC), generates acyl-CoA, which enters the TCA cycle. These enzymes have established roles in amino acid metabolism and whole-body nitrogen shuttling, in particular with respect to the *de novo* synthesis of brain glutamate (LaNoue *et al.*, 2001; García-Espinosa *et al.*, 2007; Leith *et al.*, 2001; Coles *et al.*, 2012). We have previously reported that the levels of these proteins were increased in Alzheimer's disease (AD) brain, which could contribute to the generation of excess glutamate, promoting neurotoxicity (Hull *et al.*, 2015). However, emerging new evidence has since indicated that these proteins, traditionally assigned metabolic roles, may have additional cellular 'moonlighting' functions (particularly through the P13K/mTORC1 and autophagy pathways), which are regulated through their peroxide sensitive-redox active CXXC motif (Conway and Lee, 2015).

This CXXC motif is unique to these aminotransferases (Conway *et al.*, 2002; Conway *et al.*, 2003; Conway, 2004) and when modified through oxidation (Conway *et al.*, 2002, Conway *et al.*, 2004) S-nitrosation (Coles *et al.*, 2009) or S-glutathionylation (Conway *et al.*, 2008) are reversibly inactivated. The N-terminal cysteine residue acts as a redox sensor and the second cysteine operates as the resolving cysteine, preventing irreversible oxidation. The function of this redox switch has in part been characterised for BCATm, influencing its formation of a metabolon with the E1 subunit of BCKDC (Islam *et al.*, 2007) and glutamate dehydrogenase (GDH) (Islam *et al.*, 2010), enzymes important for the complete oxidation of the BCAA. When inhibited by oxidation, BCATm no longer catalyzes transamination, preventing metabolite channeling through both its lack of activity and its decreased ability to stabilize multi-enzyme complexes. We have also shown that *in vitro* the BCAT proteins have novel thiol oxidoreductase activity that can accelerate the refolding of reduced and denatured RNase, in particular when S-glutathionylated, supporting a chaperone role for BCAT in protein folding (El Hindy *et al.*, 2014). Several other proteins, isolated from neuronal IMR32 cells, that are directly involved or controlled by G protein cell signalling and known to be modulated by peroxide were also identified as binding partners for BCAT (Coles *et al.*, 2009). While various phosphorylation sites, particular to protein kinase C (PKC) are structurally evident in BCAT,

it remains unknown if BCAT phosphorylation influences its activity or proposed moonlighting role, in particular with respect to AD pathology.

PKC, like the P13K/Akt/mTORC1 signalling pathway, regulates autophagy through key nutrient signals such as the BCAAs, insulin and nutrient deprivation (Choi *et al*., 2015; Heras-Sandoval *et al*., 2014; Zhou *et al*., 2015). Autophagy is a degradation and recycling system that removes cytoplasmic components such as misfolded or aggregated proteins through several stages that culminates with fusion of the autophagosome and the lysosome (Glick *et al*., 2010). Induced autophagy can be stimulated by changes in nutrient status, growth factors or oxidative stress, important to cell survival (Shafei and Conway, 2017). However, inhibition or disruption to the formation or clearance of the autophagosome or fusion with the lysosome can result in a shift in autophagic flux, leading to aggregate accumulation as observed in neurodegenerative conditions such as AD (Nixon *et al*., 2005). In fact, accumulation of autophagic vacuoles with high levels of amyloid β have been reported in post-mortem AD brain (Cataldo *et al*., 1997; Nixon *et al*., 2005; Nixon, 2007) and considered an early event in disease pathogenesis (Perez *et al*., 2015). Therefore, whilst autophagy is generally considered to play a role in cell survival, disruption to autophagic flux has been linked with cell death.

Inhibition of PKC using staurosporine (SS) is known to cause a loss in autophagy, whereas activation using phorbal 12-myristate 13-acetate (PMA) can promote it (Zhang *et al*., 2009). In AD models, it is known that activation of PKCα (and MAPK) promotes the production of the secretory form of amyloid precursor protein (sAPPα) (Kim *et al.,* 2011), which reduces the accumulation of pathogenic Aβ levels (Hung *et al*., 1993; Gabuzda *et al*., 1993), whereas Aβ accumulation directly inhibits PKC activation (Lee *et al*., 2004). Indeed in AD brain, levels of PKC, its receptors (Battaini *et al*., 1999; Kurmatani *et al*., 1998) or activity (Moore *et al*., 1998; Zhu et al., 2001) and associated phosphatases are decreased (Sontag and Sontag, 2014), as is autophagosome flux (Nixon *et al*., 2005; Yu *et al*., 2005; Yu *et al*., 2004), all of which have been correlated with AD pathology and possibly as a direct result of Aβ. However, the underlying mechanisms relating these pathways and how they are perturbed in AD is still unknown.

As nutrient signals and insulin drive crosstalk between these pathways, which relate to BCAT metabolism, the focus of this study was to determine if BCAT plays a fundamental role in autophagy-mediated regulation of Aβ through redox-regulated phosphorylation of BCAT. Collectively, our data support kinase-mediated phosphorylation of BCAT that is modulated by

cysteine residues and redox state, and linkage of phosphorylation state to Aβ accumulation via deregulation of autophagic flux, pointing to novel targets to regulate Aβ load in AD. In summary, subcellular translocation of BCATc is mediated through redox-regulated PKC phosphorylation, important to autophagic flux and Aβ processing.

MATERIALS AND METHODS

Materials

Protein kinase C isoforms; α, βI, βII, γ, θ, ε, η, and δ, adenosine triphosphate (ATP), phosphatase inhibitor, L-glutamic acid, L-glutathione reduced, L-glutathione oxidized, diacylglycerol, PS, protease inhibitor, iodoacetamide, N-ethyl maleimide (NEM), hydrogen peroxide, α-ketoisocaproate (KIC), α-ketoisovalerate (KIV), phenylmethanesulfonyl fluoride (PMSF), tunicamycin, chloroquine diphosphate salt, bafilomycin and rapamycin were obtained from Sigma Aldrich (Poole, Dorset, UK). Protein A/G Sepharose was purchased from Abcam (Cambridge, UK). HiTrap^{TM} Q HP and PD10 columns were obtained from GE Healthcare (Buckinghamshire, UK). γ^{32}P-ATP was obtained from Perkin Elmer (Cambridge, UK). Labelled C^{14} Valine was obtained from ARC (London, UK). Rabbit raised antibody to BCATc was raised against protein purified by this group and purchased from Insight Biotechnology Limited (Wembley, UK). All other chemicals were obtained from Fisher Scientific (Loughborough, UK) or Invitrogen (Paisley, UK).

In vitro phosphorylation of BCAT proteins with various PKC isoforms in response to altered redox condtions.

In vitro phosphorylation of BCAT proteins was assessed by incubation of BCAT with various PKC isoforms using the radioactive isotope γ^{32}P-ATP. Initially, BCAT was exchanged into 50 mM HEPES (pH 7.2), containing 0.2 mM DTT and subsequently phosphorylated in the presence of 10 mM MgCl$_2$, 10 mM ATP ($^{\gamma}$ATP), diacyl glycerol (10 mg/mL) and phosphatidyl serine (2 mg/mL) (α, βI, βII, γ, 5 mM CaCl$_2$) for 30 minutes at 30ºC. Phosphorylated BCAT was separated using 1D-SDS-PAGE (12%) and the proteins were resolved using Gel-code. The gels were subsequently vacuum-dried and imaged via digital autoradiography. As phosphorylation was optimal for PKCα, this isoform was used in all subsequent experiments. The effect of phosphorylation over time (2-30 minutes) was also determined at 30ºC. The importance of the redox-active thiol groups was established using mutant BCAT proteins (BCATc: C335S, C338S, C335/8S and BCAT: C315S and C318S) in place of wild-type proteins under the same experimental conditions.

To determine the effect of changing the redox environment on BCAT proteins, phosphorylation by PKCα, the proteins were incubated for 30 minutes with S-Nitrosoglutathione (GSNO) (1 mM), oxidised glutathione (GSSG) (1 mM) or reducing agents such as DTT (1 mM) and glutathione (GSH) (1 mM), and also the thiol inhibitor, NEM (8 mM), respectively. The BCAT

proteins were subsequently exchanged into 50 mM HEPES buffer (pH 7.2) and phosphorylated as described above. Phosphorylation then proceeded for 15 minutes at 30°C following the addition of the kinase.

In vitro dephosphorylation of BCAT proteins in a time dependent manner.

To evaluate the effect of time on dephosphorylation, BCAT proteins were exchanged into 50 mM HEPES buffer (pH 7.2) containing 0.2 mM DTT. The BCAT proteins were phosphorylated for 30 minutes at 30ºC by PKCα as described above and subsequently dephosphorylated using 2 µL of protein phosphatase 1 over 0, 5, 10, 15, 20 and 50 minutes at 30ºC. Dephosphorylation was imaged as previously described above.

Phosphorylation of BCAT proteins in human neuroblastoma cells IMR-32.

Phosphorylation of BCAT proteins in human neuroblastoma (IMR-32) cells was demonstrated by incubating cells in buffer containing 5.6 mM KCl, 0.2 mM KH_2PO_4, 137.6 mM NaCl, 2.4 mM Na_2HCO_3, 5.6 mM glucose, 0.4 mM $MgSO_4$, 0.5 mM $MgCl_2$, 20 mM HEPES (pH 7.4), 1.26 mM $CaCl_2$ and 10 mM ATP for 2 hours at 37°C at 5% CO_2. Proteins from these cells were extracted in RIPA buffer containing 10 mM Tris (pH 7.6), 150 mM NaCl, 1 mM EDTA, 1 mM EGTA, 1% triton X-100, 1X protease inhibitor and were subjected to lysis using a syringe followed by centrifugation at 10,000 X g at 4°C. Proteins were separated by 1D-SDS-PAGE (4-12% Bis-Tris gels) followed by Western blot analysis to probe for BCAT phosphorylation using an antibody which detects phosphorylation at serine residues surrounding by arginine/lysine and hydrophobic residues of PKC substrates (1/1000) (Cell Signalling, Hertfordshire, UK) and BCATc (1/1000).

Subcellular fractionation

After appropriate treatment, IMR-32/SH-SY5Y cells were washed twice in ice cold PBS prior to scraping in PBS. The cells were centrifuged for 5 minutes at 900 X G and re-suspended in Tris buffer (50 mM Tris, 150 mM NaCl, 1 X EDTA-free Protease inhibitor, pH 7.5), extracted through a G25 needle twenty times and incubated on ice for 30 minutes. To remove the nuclear fraction, the cell lysates were centrifuged at 900 X G for 5 minutes at 4°C. The supernatant was removed and centrifuged at 20,000 X G to isolate the membrane fraction from the cytosolic, which was then re-suspended in MES-buffered saline (25 mM MES, 150 mM NaCl, 1% Triton X-100™, 1 X EDTA-free Protease Inhibitor, pH 6.5) and incubated on ice for 60 minutes. After centrifugation at 20,000 X G for 30 minutes at 4°C, the non-raft membrane fraction was collected as supernatant and the raft-membrane pellet was re-suspended in Tris

buffer containing 60 mM β-octylglucoside and 1 % Triton X-100™ and incubated on ice for 30 minutes. The raft-membrane fraction was then collected as supernatant after centrifugation at 15,000 X G for 20 minutes at 4°C. Protein concentrations were calculated using the Bradford assay, the samples were separated by 4-12% SDS-PAGE followed by Western blot analysis.

Western blot analysis of proteins from IMR-32 and SH-SY5Y treatments.

Protein samples (20 µg/µL) were separated on a 4-12% SDS PAGE and transferred either a nitrocellulose or a PVDF membrane for 2 h at 50 V (low molecular weight proteins) or 18 hours at 35 V (high molecular weight proteins) in transfer buffer (20% Methanol, 25 mM Tris, 190 mM Glycine, pH 8.3). The membrane was washed three times with Tris buffered saline with Tween (TBST: 0.1% Tween, 200 mM NaCl, 2 mM Tris, pH 7.5) for 10 minutes each and blocked (with 5% non-fat milk or 5% BSA) for 1 hour. Primary antibody (5% BSA for pAkt, pmTOR and pS6K (1/1000), and in 5% non-fat milk for BCATc (1/3000), Beclin (1/1000), p62 (1/2000) and LC3 (1/500/1/1000)) was added to the membrane and incubated overnight at 4°C. After three 10-minute washes with TBST and an additional block with 5% non-fat milk for 30 minutes, secondary antibody (HRP linked) in 5% non-fat milk was added for 1 hour. Following three 10-minute washes with TBST, chemiluminescent HRP substrate was added for 1 minute and exposed to film for various time periods, or imaged using an Odyssey FC (Li-cor Biosciences, Cambridge, UK).

Confirmation of palmitoylation of BCATc

SH-SY5Y cells were transferred to EBSS for 1 hour and subsequently treated with 10 µM tunicamycin +/- 100 nM insulin for 2 hours in EBSS. Cells were washed twice in ice-cold PBS and scraped in lysis buffer (LB – 1% IGEPAL CA-630, 150 mM NaCl, 10% glycerol, 10 mM PMSF, 50 mM Tris-HCl, pH 7.5) containing protease cocktail inhibitor + 50 mM NEM. Cells were collected in pre-cooled 1.5 mL centrifuge tubes and sonicated for 15 seconds on ice, before nutating for 30 minutes at 4ºC. Cell lysates were subsequently centrifuged at 16 000 x g for 30 minutes and supernatant collected into a new pre-cooled 1.5 mL centrifuge tube. Protein concentration was measured using the Bradford assay. BCATc primary antibody was added to the cell lysates, and incubated overnight at 4ºC.

Following overnight incubation, 60 µL of protein A/G-coated sepharose beads were added to each sample and incubated for 1 hour at 4ºC. Lysates were centrifuged at 0.5 x g for 1 minute at 4ºC, the supernatant removed and the pellet resuspended in 600 µL LB + 10 mM NEM. Following resuspension, 200 µL of sample were added to pre-cooled tubes labelled –HAM

with an additional 300 µL of LB + 10 mM NEM. The remaining 400 µL were added to +HAM tubed with 100 µL LB + 10 mM NEM, and all samples were incubated on ice for 10 minutes. Samples were quickly washed with 0.5 mL stringent buffer (10 mM NEM, 0.1% SDS in LB), following three washes with 0.5 mL LB, pH 7.2 and 0.5 x g for 1-minute spins between washes. 0.5 mL of LB pH 7.2 were added to each –HAM sample, and 0.5 mL of LB pH, 7.2 with 1 M HAM were added to +HAM samples. These were allowed to react for 1 hour at room temperature.

Beads were gently washed with LB pH 6.2 to remove residual HAM buffer, prior to supernatant being removed and samples incubated on ice. 0.5 mM of Biotin-BMCC buffer (2.5 µM Biotin-BMCC solution in LB pH 6.2) were added to each sample and these were reacted for 1 hour at 4ºC. Following incubation, samples were gently washed once with LB pH 6.2 and three times with LB pH 7.5 + PMSF and protease inhibitor. Supernatant was then removed and any remaining buffer collected underneath the bead slurry was carefully removed. Proteins were separated using 4-10% SDS PAGE.

Regulation of BCAT subcellular translocation

To evaluate the effect of changes in the redox environment on BCATc translocation, SH-SY5Y cells were incubated with 100 µM and 1000 µM H_2O_2, respectively, relative to reduced conditions using 10 mM DTT. Proteins were subsequently extracted and analysed using subcellular fractionation and Western blot analysis as described above. As leucine is a key nutrient signal, it may play an important role in recruiting BCATc to the membrane. SH-SY5Y cells were grown in EBSS for one hour, and treated with 5 mM, 10 mM or 20 mM leucine or glutamate, respectively or 100 nM insulin and then analysed using subcellular fractionation followed by Western blot analysis. To determine the effect of PKC activation or inhibition on translocation of proteins to the cell membrane, cells were incubated in EBSS for 1 hour and then treated for 3 hours with 200 nM PMA (PKC activator) or 2.3 nM Go6976 and 3 nM staurosporine (PKC inhibitor) +/- 100 nM insulin, and analysed using subcellular fractionation followed by Western blot analysis.

Confocal microscopy of BCATc under varied redox or nutrient conditions

SH-SY5Y cells were allowed to reach 70%–80% confluence and treated under various redox (+ / - hydrogen peroxide (100 µM or 1000 µM) or +/- DTT (10 mM)) for 30 min, respectively, at 37°C in a humidified incubator that was adjusted to contain 5% CO_2. In a separate experiment SH-SY5Y cells were grown in EBSS for one hour, and treated with 100 nM insulin

or 100 nM rapamycin for 30 minutes. After serial washes, the cells were fixed with 0.25% glutaraldehyde and permeabilized with 0.2% Triton X-100 for 20 minutes at RT in a 0.1 M sodium cacodylate buffer, pH 7.4 adjusted to contain 0.1 M sucrose. The cells were further treated by a succession of washes with sodium borohydride (1 mg/ml in PBS) and blocked in 3% BSA overnight before incubating with primary antibodies, anti-BCATc, (1/500), anti-Vps34, anti-LC3 and anti-4EBP1 (1/150 dilution), respectively, for 1 h at RT. After serial washes, the cells were incubated with goat anti-rabbit Alexa Fluor-568 or goat anti-mouse Alexa Fluor 488 for 1 h at RT. Slides were washed in cacodylate buffer and mounted in 300 nM DAPI in glycerol. The Mander's correlation coefficients (Mx and My) were derived using Volocity (Perkin-Elmer) from an average of 15 individual cell images.

Autophagy analysis using bafilomycin and chloroquine

For autophagy assessment, SH-SY5Y cells were maintained in culture to approximately 80% confluence, and subsequently nutrient deprived in EBSS for 3 hours. Cells were treated with 100 nM rapamycin, 100 nM bafilomycin or 50 µM chloroquine for 30 minutes, leucine deprived for 3 hours. Protein was extracted from whole cells by scraping in RIPA buffer (25 mM Tris, 150 mM NaCl, 1 mM EDTA, 0.5 mM EGTA, 1 mM NaF, 1 mM PMSF, 1 x phosphatase inhibitor, 1 x protease inhibitor, pH 7.6) containing 0.01% Triton X-100, and quantified using the Bradford assay. Samples were analysed by Western blot analysis using antibodies against BCATc (1/3000), LC3 (1/1000) and p62 (1/2000).

Knockdown and overexpression of BCATc in SH-SY5Y and autophagy assessment

Knockdown (autophagy): SH-SY5Y cells were seeded into 6-well plates and immediately transfected with 20 nM BCATc siRNA, following optimisation from the manufacturer's protocol (Lipofectamine™ RNA iMAX, Thermo Fisher Scientific, Waltham, MA, USA). Cells were incubated for 24, 48, and 72 with media changed after 24 h for longer incubation times. Proteins from whole cell extracts were separated on 4-12% SDS PAGE followed by Western blot analysis as described.

Overexpression of BCATc and autophagy (subcellular fractionation): Cells were seeded at highest confluency in 75 mm^2 culture flasks and allowed to attach overnight. BCATc was overexpressed by preparing 10 µg total BCATc plasmid DNA and 30 µg polyethylenimine (PEI – 1:3 DNA to PEI ratio (w/v)) in Opti-MEM, incubating complex for 15 minutes and adding to cells for a total of 72 h, including a 24 h post-transfection medium change. Cells were nutrient deprived for 1 hour and treated for 3 hours with PKC inhibitors staurosporine (3

nM) and Go6976 (2.3 nM), PKC activator PMA (200 nM) and/or 100 nM insulin, respectively, prior to subcellular fractionation.

Effects of overexpressed BCATc on Aβ levels: Cells were overexpressed with 0.5, 1.0, 1.5 and 2.5 µg of BCATc with jetPRIME® following the manufacturers' protocol (Polyplus Transfection, New York, NY) +/- insulin or leucine. In brief, cells were seeded in 6-well plates at a density of 2×10^6 cells/well and allowed to attach overnight. Transfection reagent and increasing concentrations of DNA plasmid (1:2 DNA to jetPRIME® ratio (w/v)) were prepared in reduced-serum media (Opti-MEM), incubated for 15 minutes at RT and subsequently added to wells. Cells were incubated with transfection complex for 24 hours before medium change, and to a total of 72 h prior to extraction with RIPA buffer (10 mM Tris-HCl, 150 mM NaCl, 1 mM EDTA, 1 x protease inhibitor, pH 7.5) and Western Blot analysis (Primary antibodies: BCATc 1:3000, LC3 1:1000, Aβ 1:1000).

RESULTS

The redox-active CXXC motif of BCAT regulates PKC phosphorylation.

The BCAT proteins have various phosphorylation motifs as defined using the Motif Scan program (http://scansite.mit.edu) (Figure 1A), highlighting 3 structurally accessible consensus sequences for PKC, (BCATc) T24, T36 and T128 and (BCATm) S30, S31 and T59 (Figure 1B). Conventional and atypical isoforms of PKC were used to phosphorylate BCAT using the radioactive isotope γ^{32}P-ATP and those that are calcium, diacyl glycerol and phosphatidylserine dependent show increased γ^{32}P-ATP incorporation relative to δ, ε, θ and η (Figure 1C). Reversible phosphorylation by PKCα and phosphatase 1, respectively changed in a time dependent manner and followed a bi-phasic pattern (Figure 1D (i-iv)), which may be explained by the accessibility of the phosphorylation sites.

To assess the role of cysteine residues in regulating phosphorylation, the CXXC mutants (C335S, C338S and C335/8S for BCATc and C315S, C318S for BCATm) were tested for their ability to act as targets for PKCα. Mutation of the thiol groups of the CXXC motif Cys to Ser significantly reduced PKC phosphorylation (Figure 2A). For both isoforms, the N-terminal cysteine residues appears to be more critical for phosphorylation, indicating that the redox sensor at position C315 or C335 is essential for phosphorylation. The importance of the thiol groups to PKC phosphorylation was established using the thiol specific inhibitor NEM, which completely inhibited BCAT phosphorylation (Figure 2B). Incubation of BCATc with the reducing agent DTT and the physiologically relevant reducing agent GSH resulted in an increase in phosphorylation (Figure 2B). Conversely, incubation with GSSG and GSNO significantly reduced BCATc phosphorylation relative to reduced protein (Figure 2B). Interestingly, although NEM abolished phosphorylation of BCATm, supporting the role of these thiol groups in this mechanism, incubation with GSNO or GSSG did not prevent PKC phosphorylation, indicating that the underpinning mechanisms of redox-regulated phosphorylation differs between isoforms. Treatment of human neuroblastoma (IMR32 cells) PMA resulted in the phosphorylation of target proteins (Figure 2C(i)). Proteins were extracted from cells, and analysed by Western blot analysis using antibodies specific for phosphorylation and BCATc. Phosphorylated protein at the expected molecular weight for BCATc was confirmed (Figure 2C(ii)). Overlay of cellular phosphorylation with BCATc supports that BCATc is a target for PKC phosphorylation in cells (Figure 2C(iii)).

Translocation of BCATc to the membrane through S-palmitoylation is regulated by changes in the cellular redox environment

Previous studies demonstrated that it is the redox state of the BCAT proteins that supports binding of proteins involved in G-protein cell signalling (Coles *et al*, 2009). PKC targets are often associated with the membrane, but BCATc is normally distributed in the cytosol. However, we showed using fractionation studies that pools of BCATc exist, in the membrane and nuclear fractions (Figure 3A). Fraction purity was confirmed using subcellular specific proteins Na^+, K^+-ATPase and Hsp90. BCATc has several palmitoylation sites (Figure 3B), which can undergo palmitoylation as evidenced by the Acyl-Biotin assay +/- tunicamycin (Figure 3C). These pools of BCATc were found to be regulated in response to changes in the redox environment (Figure 3D). In response to oxidation (Figure 3D(i)) the pool of BCATc at the membrane increased, whereas in response to DTT the accumulated pool was significantly decreased (Figure 3D(ii)). Here, we propose that BCATc docks at the membrane in response to changes in cellular redox status. Notably, an increase in nuclear BCATc was also observed.

PKC activation and BCAT substrates regulate membrane localisation of BCATc

Leucine is a key nutrient signal and works in synergy with insulin-mediated signalling. However, the role of BCATc in this pathway is not entirely clear. We next evaluated if insulin or BCAA substrates effect BCATc trafficking through a PKC-mediated pathway. In response to insulin there was an increase in BCAT recruited to the membrane (Figure 4A). On the other hand, leucine and glutamate showed a dose-dependent decrease in membrane bound BCATc (Figure 4B (i and ii)) indicating that BCATc trafficking is regulated through hormonal triggers and nutrient status. Moreover, inhibition of PKCα using staurosporine caused a significant increase in membrane BCATc that was further enhanced with insulin (Figure 4C). This data indicates that BCATc translocation to the membrane is regulated through an insulin/PKCα-mediated mechanism.

BCAT regulates autophagy through PKC-mediated interactions.

Leucine, the BCAT substrate, is known to activate mTORC1 and inhibit autophagy, however, less is known about the role of BCATc in this mechanism. We first showed that the level of BCATc increased in response to nutrient-deprivation or rapamycin (Figure 5A (i and ii). Not only did the level of BCATc increase but so too did its association with Vps34, in particular at the cell membrane where, based on the Mander's correlation coefficient, these proteins colocalise. Using other markers of autophagosome synthesis such as Beclin, and LC3, we confirm that in response to leucine deprivation (LD) that the level of BCATc significantly increased, as did Beclin and LC3I lipidation (Figure 5B (i)). The increase in both of these

markers suggests that autophagosome synthesis is increased, which will impact flux dependent on clearance. Using the inhibitors Bafilomycin (inhibits acidification and fusion) and chloroquine, (inhibits fusion) accumulation of LC3II and p62/Sequestosome1 (SQSTM1) was associated with increased levels of BCATc (Figure 5C), indicating that BCATc is integral to autophagosome synthesis.

Knockdown of BCAT1 showed a related loss in both LC31 lipidation and levels, also observed for p62 (Figure 5D(i)). Using whole cell extracts we then showed that knockdown of BCAT1 increased the levels of pAkt, pmTORC1 and p4EBP1, dependent on the level of BCATc (Figure 5D (ii)). This suggest that BCATc is not only important in regulating autophagy but may also play a role in the P13K/Akt/mTORC1 axis, potentially facilitating crosstalk between these signalling pathways. We next examined the response of LC3I lipidation in cell fractions with overexpressed BCAT (as observed in AD brain) to treatment with insulin and PKC regulation. Cells overexpressing BCATc showed increased levels of LC3I predominantly in the membrane and nuclear fraction relative to untransfected cells (Figure 5E). Moreover, BCATc-induced autophagy was regulated by PKC activity, with increased lipidation observed when PKC was inhibited (Figure 5E(ii)). This indicates that BCATc-induced autophagy is regulated through cycles of PKC activation and inhibition, serving as a regulatory switch in autophagy control. In our studies we also show that overexpression of BCATc alone increased nuclear levels of LC3I, as did activation of PKCα (Figure 5E (iii)), indicating that BCATc regulates autophagy at several points of the autophagy pathway.

Overexpressed BCATc regulates Aβ levels, which leucine controls.

Our group have reported that BCATc is increased in AD brain (Hull *et al*., 2015). To evaluate the impact of BCATc on Aβ processing we investigated if increased levels of BCATc regulated Aβ load through autophagy. Here we show that sustained overexpression of BCATc resulted in a dose-dependent increase in autophagy with a concomitant increase in the levels of Aβ (Figure 6A). However, as the level of BCATc and autophagosome formation increased, the amount of intracellular Aβ eventually decreased, indicating that Aβ processing, controlled through BCATc-mediated autophagy was compromised. Our confocal microscopy analysis shows that cells with this increased BCAT expression are less uniform and subject to neuronal cell death (Figure 6B). The observed increase in autophagy was sustained in response to insulin but reduced when incubated with leucine, together with a striking decrease in Aβ, indicating

that despite BCATc-induced autophagy, leucine signalling can over-ride BCATc-induced Aβ accumulation, offering a novel target to modify Aβ load.

DISCUSSION

There is a regional increase in the BCAT proteins in AD brain, which correlated with an increase in Braak stage, supporting a role for BCAT in AD pathology (Hull *et al*., 2015). Whilst their role in regulating brain glutamate is well established (reviewed in Conway, 2019, in press) the importance of the CXXC regulatory switch has yet to be evaluated in this context. Based on affinity-tagged metabolic studies we have suggested that BCAT has multiple roles in the cell, dependent on its redox state (El Hindy and Conway, 2019 and Conway and Lee, 2015). Relevant to this discussion is the redox regulated association of BCATc with proteins involved in G protein cell signalling and autophagy (Conway *et al*., 2008). Here, we show that calcium, diacyl glycerol and phosphatidylserine dependent PKC kinases (Dempsey *et al*., 2000) have increased γ^{32}P-ATP incorporation relative to δ, ε, θ and η (Figure 1C). PKCɣ, solely expressed in the brain and spinal cord, and restricted to neurons (Saito *et al.*, 2002), significantly increased γ^{32}P-ATP incorporation for BCATc (Hull *et al*., 2012). While PKC isoforms in this group have conserved domains, there are slight differences in the tertiary structure, especially in the catalytic domain, which may account for various degrees of BCAT phosphorylation (Steinberg *et al*., 2008, Steinberg, 2015). The phosphorylation sites in BCAT have one of the three basic amino acids, arginine (K), histidine (H) or lysine (R) that may also facilitate this binding as will the XX dipeptide of the CXXC motif (Yennawar *et al*., 2006; Goto *et al*., 2005).

Here, initial phosphorylation may cause a conformational change that increases access to other sites or could be due to the basic residues adjacent to the target site, a pattern also described for PKCα activation of T cells (Houtman *et al.*, 2004; Cruz-Orcutt *et al*., 2014). For both isoforms, we show that the accessible thiols are critical for PKCα phosphorylation, more dominant with the N-terminal mutant (Figure 2A). Incubation of BCATc with GSSG or GSNO reduced phosphorylation but had no impact on BCATm (Figure 2B). This differential regulation of BCAT isoforms by GSNO and S-glutathionylation was previously reported (Coles *et al*., 2009) and may be in part due to the increased redox sensitivity of BCATc compared to BCATm, where their regulation through phosphorylation could point to different signalling roles in the cell (Cole *et al*., 2012). In related studies, protein S-glutathionylation of neurogranin and neuromodulin through GSNO-mediated interactions showed that modification of the reactive thiols rendered neurogranin a poorer substrate for PKC (Li *et al*., 2001). The reduced substrate specificity by oxidised BCAT for PKCα is most probably due a conformational shift and availability of the phosphorylation site, as described for rat brain

neurogranin (Sheu *et al*., 1996; Miao *et al*., 2000). Additionally, PKCα has cysteine rich motifs that are also redox active (Gopalakrishna *et al.*, 2000; Gopalakrishna *et al.*, 2008), which indicates that redox control will be pivotal to the interplay between these two proteins.

Translocation to membranes traditionally has been considered the hallmark of PKC activation, but typically, BCATc resides in the cytosol. However, we showed using fractionation studies that pools of BCATc exist, in the membrane and nuclear fractions (Figure 3A). Membrane association can occur through protein lipidation, which regulates cell response to nutrient signals such as those cited and not only modulates protein localisation but also enzyme activity and protein:protein interactions (Spinelli *et al*., 2018). The main protein acylations include myristoylation, prenylation, and palmitoylation, the latter is the only reversible fatty acylation (specifically S-palmitoylation), regulated by palmitoyl acyltransferases (Linder and Deschenes, 2004). BCATc has several palmitoylation sites (Figure 3B), which can undergo palmitoylation as evidenced by the Acyl-Biotin assay +/- tunicamycin (Figure 3C). Moreover, BCATc was also identified as a binding partner to palmitoyl protein thioesterase (PPT, resides in lysosomes) and acyl CoA thioesterase (APT, resides in the cytoplasm) (Duncan and Gilman, 2002; Kong *et al*., 2013), proteins which remove thioester-linked groups such as palmitate from modified cysteine residues in proteins or during lysosomal degradation (unpublished observation). We propose that BCATc is a target for cycles of acylation and deacylation, which is linked to PKC-mediated phosphorylation either at the cell or lysosomal membrane. These pools of BCATc were also found to be regulated in response to changes in the redox environment (Figure 2D) indicating that these posttranslational modifications are interdependent on PKC phosphorylation, which will be important in regulating the cellular roles of BCATc.

Leucine and insulin are key nutrient signals important in regulating protein synthesis and autophagy. Insulin is the most potent anabolic hormone known, with wide-ranging targets notably essential for maintaining glucose homeostasis through translocation of the glucose transporter GLUT4 isoform to the cell surface via a signalling cascade involving P13K/Akt (Pessin and Saltiel, 2000). Insulin has also been shown to have novel S-palmitoylation targets such as platelet-activating factor acetyl hydrolase IB subunit gamma, which loses its role in cell migration once S-palmitoylated (Wei *et al*., 2014). Here, we propose that BCATc docks at the membrane in response to changes in cellular redox status or insulin signalling through S-palmitoylation and is released through phosphorylation by PKCα (as PKCα activation

reduces the pool of membrane bound BCATc, Figure 4C). As previously discussed, it is known that activation of PKCα promotes the production of the secretory form of sAPPα, which reduced the accumulation of pathogenic Aβ levels (Hung *et al*., 1993; Gabuzda *et al*., 1993). Moreover, overexpression of PKCε stimulates the activity of endothelin-converting enzymes that coincidentally have functions as Aβ-degrading enzymes beyond their vasomodulatory roles (Choi *et al*., 2006). As the levels of PKC and phosphatases are decreased in AD brain, it could potentially increase the pool of membrane bound BCATc impairing its cycling to the cytosol. Given the increased levels of BCAT in AD brain, this could alter other suggested moonlighting functions for BCAT such as regulation of the P13K/Akt/mTORC1 and autophagy-mediated pathways (Conway and Lee, 2015).

Whilst autophagy is fundamental to maintaining brain health, excessive or imbalanced, autophagy can lead to autophagosome or aggregate accumulation contributing to neurodegenerative conditions such as AD (Button *et al*., 2017). Accumulation of autophagosomes may result from an increase of autophagosome synthesis, disruption of autophagosome-lysosome fusion/clearance or both. We first showed that the level of BCATc increased in response to nutrient-deprivation or rapamycin together with Vps34 (Figure 3A (i and ii)), a positive regulator of autophagy and inhibitor of mTORC1 (Chen *et al*., 2014). Using other markers of autophagosome synthesis such as Beclin, important for nucleation (Itakura *et al*., 2008), and LC3, a key protein in autophagosome synthesis (Brier *et al*., 2019), we confirm that increased BCATc, in response to leucine deprivation, corresponds to an increase in these autophagy markers that are integral to autophagosome synthesis. This was confirmed using the inhibitors bafilomycin, a vacuolar H^+ ATPase-inhibitor (used to assess autophagic flux, Mauvezin *et al*., 2015) and chloroquine (inhibitor of autophagosome and lysosome fusion, Mauthe *et al*., 2018)), which show an accumulation of LC3II and an associated increase in BCATc (Figure 3C). p62/Sequestosome1 (SQSTM1), a multifunctional scaffold protein that acts as a receptor that binds and delivers poly-ubiquitinated proteins to the UPS or to the autophagosome for degradation, was also elevated. A role for BCAT in autophagy regulation was confirmed with knockdown of BCAT1, which showed a related loss in both LC31 lipidation and levels, also observed for p62 (Figure 3D(i)). The effect of BCAT1 knockdown also affected proteins important to the P13K/Akt/mTORC1 axis indicating that BCATc, facilitates crosstalk between these signalling pathways. Conversely, overexpression of BCATc, as observed in AD brain, increased autophagy, regulated by PKC. Collectively, these data suggest that BCATc is important to autophagosome synthesis and potentially flux,

dependent on the rat of clearance. However, since a decrease in p62 is characteristically associated with enhanced degradation of the autolysosome (Flores-Bellver *et al*., 2014), a role for BCATc in autophagosome synthesis is likely.

Although autophagy is largely reported as a cytoplasmic event, its role in transcriptional and epigenetic regulation in the nucleus is gaining support, in particular in situations of prolonged starvation (reviewed in Baek and Kim, 2017). Several regulators of histone modification, which have the potential to activate or repress transcription factors have also been cited as key modulators of autophagy. These include, but are not limited to coactivator-associated arginine methyltransferase 1 (CARM1, also called protein arginine methyltransferase 4 (PRMT4)), and H3R17 methyltransferase (Shin *et al*., 2016). Notably, amino acid depletion or treatment with rapamycin, both of which increase BCATc and autophagy, stimulate activation of CARM1, which results in histone H3R17 dimethylation. Interestingly, BCAT binds CARM1 and although the impact of this association is unknown, we propose that it might facilitate its activation in response to nutrient deprived conditions. In our studies we show that overexpression of BCATc alone increased nuclear levels of LC3I, as did activation of PKCα (Figure 3E, lower panel). Nuclear LC3 is abundant and considered to act as a reserve for the cytoplasmic pool during autophagy or is alternatively involved in non-autophagy events (Huang *et al*., 2015). The increase in nuclear LC3 in response to overexpressed BCATc could be a signal to increase the residual stores for autophagy. Our data points to several pools of activated BCATc where their cellular distribution, determined through their redox-regulated phosphorylation, can potentially contribute to autophagy regulation at several sites.

A focus of this research was to better understand the impact of BCAT overexpression on AD pathology. Overexpression of BCATc caused increased autophagy together with increased levels of Aβ, supporting a role for BCAT in regulating Aβ clearance. Addition of leucine altered autophagic flux and prevented Aβ accumulation, highlighting the importance of nutrient signals in regulating metabolic pathways linked with Aβ processing. Previously, we proposed that BCATc was initially increased in a neuroprotective capacity, however, sustained increase could lead to the protein shifting from neuroprotective to neurotoxic if glutamate levels accumulated (Hull *et al*., 2015). However, the role of the CXXC motif was not considered in this model. It is widely accepted that oxidative and nitrosative stress is a feature of neurodegenerative conditions (Nakamura and Lipton, 2009), which will alter the activity and function of BCAT, dependent on the modification and subsequent phosphorylation. To add to

the complexity, one must also consider the nutrient and hormone signals, which are also perturbed in AD. The BCAAs show significant changes in their profile between individuals with mild-cognitive impairment and AD patients relative to healthy age-related controls (Hudd *et al*., 2019), which based on our findings could contribute to ineffective clearance of Aβ.

In summary, we propose that pools of BCATc exist and subcellular translocation is mediated through redox-regulated phosphorylation that alters autophagic flux (Figure 7). First, in response to nutrient signals such as leucine deprivation or insulin, BCATc associates with the membrane through palmitoylation. Association with the membrane is regulated through phosphorylation, where PKC phosphorylation at T24 or T36 signals BCAT to disengage. Second, the expression of BCATc is important for autophagosome synthesis, where increased or decreased levels of BCATc is associated with a corresponding increase or decrease in markers of autophagosome synthesis such as LC3 and Beclin. Third, in response to increased levels of BCATc, as observed in AD, Aβ levels accumulate due to a shift in autophagic flux, which is attenuated when incubated with leucine. In AD brain, we propose that as PKC activation decreases, regulation of BCATc-mediated autophagy is compromised leading to increased synthesis of autophagosomes that could contribute to Aβ accumulation. Our data suggests a novel and exciting mechanism by which Aβ accumulation might be altered (through BCAAs like leucine), but subject to a better understanding of the role of nutrient signals such as the BCAAs.

ACKNOWLEDGEMENTS 21

Declaration of Interests

There are no conflicts of interest.

FIGURE LEGENDS

Figure 1. PKC phosphorylation of BCAT. For all phosphorylation reactions the BCAT proteins were incubated with the respective PKC isoform (under conditions described in materials and methods) at 30°C for 30 minutes and assessed for the incorporation of γ^{32}P-ATP using digital autoradiography**.** Upper panel: BCAT stained with gelcode and Lower panel: Radiolabelling of BCAT with γ^{32}P-ATP catalysed by PKC. Densitometry analysis: ImageJ **(PANEL A)** Putative phosphorylation sites for BCAT: The BCAT protein sequence (accession # ECA39 (BCATc) and EC2.6.1.42 (BCATm) was analysed using the Motif Scan program (http://scansite.mit.edu).   **(PANEL B)** X-RAY crystallography analysis of BCAT PKC phosphorylation sites **(PANEL C)** Phosphorylation of the BCAT proteins with PKC isoforms **(PANEL D)** PKCα phosphorylation (i and ii) and phosphatase A dephosphorylation (iii and iv) of BCAT. (Data are the mean ± SEM, N=3).

Figure 2.   Interdependence of redox-regulated phosphorylation of BCAT. Phosphorylation of BCAT and their respective mutants by PKCα was carried out at 30°C for 30 minutes and assessed for the incorporation of γ^{32}P-ATP using digital autoradiography**.** Upper panel: BCAT stained with gelcode and Lower panel: Radiolabelling of BCAT with γ^{32}P-ATP **(PANEL A)** Mutation of the redox sensor abolishes phosphorylation: BCAT and their respective thiol mutant proteins **(PANEL B)** In parallel, the BCAT proteins were incubated with DTT (10 mM), NEM (8 mM), GSNO (1 mM), GSH (1 mM) and GSSG (1 mM), respectively. The relative phosphorylation was analysed as described in Material and Methods **(PANEL C)** The proteins from IMR-32 cells were phosphorylated by native kinases under conditions described in materials and methods and analysed using 2D SDS PAGE and Western blot analysis (i) Cell protein phosphorylation using Phospho-(Ser) PKC Substrate Antibody (1/1000) (ii) Western blot analysis of BCATc (1/3000) (iii) Overlay of A and B (Data are the mean ± SEM, N=3).

Figure 3:   Translocation of BCATc to the membrane through S-palmitoylation is regulated by changes in the cellular redox environment. **(PANEL A)** Cellular pools of BCAT in IMR-32 and SH-SY5Y cells were established using subcellular fractionation: Western blot analysis of BCATc in nuclear, cytosolic and cell membrane (+/-lipid raft) fractions. **(PANEL B)** Putative S-palmitoylation sites for BCAT: The BCAT protein sequence was analysed using the Motif Scan program (http://scansite.mit.edu). **(PANEL C):** S-palmitoylation of BCATc: The Acyl-Biotin assay +/- tunicamycin. **(PANEL D)** Redox regulated trafficking of BCAT to membrane and nuclear fractions (i) Western blot analysis of

proteins from SH-SY5Y cells treated with 100 and 1000 µM H_2O_2 or (ii) 10 µM DTT for 30 mins prior to subcellular fractionation. (iii) Using confocal microscopy, SH-SY5Y cells were treated with 100 and 1000 µM of hydrogen peroxide for 30 minutes, respectively, and fixed for immunostaining as described in materials and methods, using anti-BCATc (1/250 dilution) (Data are the mean ±SEM, N=3, (*) $p \leq 0.05$, (**) $p \leq 0.001$).

Figure 4: Regulation of BCATc translocations SH-SY5Y cells were grown in EBSS for one hour, and treated with 5 mM, 10 mM or 20 mM leucine or glutamate, respectively or 100 nM insulin and then analysed using subcellular fractionation followed by Western blot analysis. The effect of PKC activation and inhibition was also assessed. **(PANEL A)** Insulin stimulation of SH-SY5Y cells: (i) Western blot analysis of membrane bound BCATc in response to insulin. (ii) In parallel, cells were fixed for immunostaining as described in methods using anti-BCATc-1 (1/250 dilution). **(PANEL B)** Leucine and glutamate regulate the membrane pool of BCATc (i) Treatment with leucine. (ii) Treatment with glutamate. **(PANEL C):** PKCα regulates trafficking of BCATc to the membrane: SH-SY5Y cells were grown in EBBS for 1 hour and treated with either 100 nM insulin, 200 nM PMA (PKCα activator) +/- insulin or 2.3 nM Go6976 and 3 nM staurosporine (PKCα inhibitors) in EBSS +/- insulin, respectively for 3 hours followed by subcellular fractionation. Western blot analysis of membrane and cytosolic BCATc (Data are the mean ±SEM, N=3, (*) $p \leq 0.05$, (**) $p \leq 0.001$).

Figure 5: BCATc regulates autophagy. SH-SY5Y cells were nutrient deprived in EBSS for 3 hours. Cells were treated with 100 nM rapamycin, 100 nM bafilomycin or 50 µM chloroquine for 30 minutes, leucine deprived for 3 hours. The effect of BCATc knockdown or overexpression on autophagy in whole cell fractions and subcellular fractions was also assessed. Proteins were extracted and analysed by Western blot analysis (Primary antibodies (BCATc (1/3000), LC3 (1/1000), p62 (1/2000) and Beclin (1/1000) and confocal microscopy as described in Materials and Methods. **(PANEL A)** (i) SH-SY5Y cells were grown on glass coverslips and treated with 100 nM rapamycin for 30 mins relative to nutrient deprived (ND) cells in EBSS for 3 hours. The cells were fixed in 0.25% glutaraldehyde for immunostaining and probed with anti-BCATc (1:500) and anti-Vps34 (1:100) for 1.5 hours and then with anti-mouse Alexa Fluor 488 (1:250) and anti-rabbit Alexa Fluor 568 (1:250) for 1.5 hours. The coverslips were then mounted and imaged using a Zeiss Axiovert 200 confocal microscope. The Mander's correlation coefficients (Mx) were derived using Volocity (Perkin-Elmer) Blue-DAPI; Green-BCATc; Red-Vps34. (ii) As described above SH-SY5Y cells were nutrient

deprived for 3 hours and probed for BCATc (green) and 4EBP1 (red). **(PANEL B)** (i) Western blot analysis of proteins from Leucine deprived (LD) cells probed for BCATc, Beclin and LC

3, respectively. **(PANEL C)** Western blot analysis of proteins extracted from SH-SY5Y cells treated with rapamycin (100 nM), bafilomycin (100 nM) and chloroquine (50 μM), respectively, and probed for BCATc, p62 and LC3. **(PANEL D)** Western blot analysis of BCAT1 knockdown (KD) relative to (i) LC3, p62 (ii) pAKT, p4EBP1 and pmTORC1 (all 1/1000)**. (PANEL E)** SH-SY5Y cells (+/- overexpressed (OE BCATc) were grown in EBBS for 1 hour and treated with either 100 nM insulin, 200 nM PMA (PKCα activator) +/- insulin, 2.3 nM Go6976 and 3 nM staurosporine (PKCα inhibitors) in EBSS =/- insulin, for 3 hours followed by subcellular fractionation. Western blot analysis of (i) cytosolic, (ii) nuclear and (iii) membrane-bound BCATc relative to LC3. (Data are the mean ±SEM, N=3, (*) $p \leq 0.05$, (**) $p \leq 0.001$).

Figure 6: Leucine reverses BCATc-induced autophagy. SH-SY5Y cells were overexpressed with 0.5, 1.0, 1.5 and 2.5 µg of BCATc +/- insulin or leucine. Proteins were extracted and analysed by Western Blot analysis (Primary antibodies: BCATc 1:3000, LC3 1:1000, Aβ 1:1000) and confocal microscopy. **(PANEL A)** Western blot analysis of proteins from SH-SY5Y cells with overexpressed BCATc under insulin and Leucine treated conditions probed for BCATc, LC3, Aβ, respectively. **(PANEL B)** (i) SH-SY5Y cells were grown on glass coverslips +/- overexpressed BCATc. The cells were fixed in 0.25% glutaraldehyde for immunostaining and probed with anti-BCATc (1:500) and anti-LC3 (1:100) for 1.5 hours and then with anti-mouse Alexa Fluor 488 (1:250) and anti-rabbit Alexa Fluor 568 (1:250) for 1.5 hours. The coverslips were then mounted and imaged using a Zeiss Axiovert 200 confocal microscope. Blue-DAPI; Green-BCATc; Red-LC3. (Data are the mean ±SEM, N=3).

Figure 7 The role of BCATc in autophagy. Inhibition of PKC activation, a change in redox or nutrient deprivation promotes translocation of BCATc to the membrane via palmitoylation. BCATc is important in regulating autophagosome synthesis affecting autophagic flux, either through nuclear regulation or autophagosome sequestration. Activation of PKC releases BCATc from the membrane and disrupts autophagic flux. Overexpression of BCATc increases autophagic flux and increases the level of intra-cellular Aβ.

REFERENCES

1. Baek SH, Kim KI. Epigenetic Control of Autophagy: Nuclear Events Gain More Attention. Mol Cell.;65(5):781-785, 2017.
2. Battaini F, Pascale A, Lucchi L, Pasinetti GM, Govoni S. Protein kinase C anchoring deficit in postmortem brains of Alzheimer's disease patients. Exp Neurol.;159(2):559-64, 1999.
3. Brier LW, Ge L, Stjepanovic G, Thelen AM, Hurley JH, Schekman R. Regulation of LC3 lipidation by the autophagy-specific class III phosphatidylinositol-3 kinase complex. Mol Biol Cell.;30(9):1098-1107, 2019.
4. Button RW, Roberts SL, Willis TL, Hanemann CO, Luo S. Accumulation of autophagosomes confers cytotoxicity. J Biol Chem.;292(33):13599-13614, 2017.
5. Cataldo AM, Peterhoff CM, Troncoso JC, Gomez-Isla T, Hyman BT, Nixon RA. Endocytic pathway abnormalities precede amyloid beta deposition in sporadic Alzheimer's disease and Down syndrome: differential effects of APOE genotype and presenilin mutations. Am J Pathol. 157(1):277-86, 2000.
6. Chen R, Zou Y, Mao D, Sun D, Gao G, Shi J, Liu X, Zhu C, Yang M, Ye W, Hao Q, Li R, Yu L. The general amino acid control pathway regulates mTOR and autophagy during serum/glutamine starvation. J Cell Biol.;206(2):173-82, 2014.
7. Choi DS, Wang D, Yu GQ, Zhu G, Kharazia VN, Paredes JP, Chang WS, Deitchman JK, Mucke L, Messing RO. PKC epsilon increases endothelin converting enzyme activity and reduces amyloid plaque pathology in transgenic mice. Proc Natl Acad Sci U S A.;103(21):8215-20, 2006.
8. Choi SW, Song JK, Yim YS, Yun HG, Chun KH. Glucose deprivation triggers protein kinase C-dependent β-catenin proteasomal degradation. J Biol Chem.;290(15):9863-73. 2015.
9. Cole JT, Sweatt AJ, Hutson SM. Expression of mitochondrial branched-chain aminotransferase and α-keto-acid dehydrogenase in rat brain: implications for neurotransmitter metabolism. Front Neuroanat.;6:18, 2012.
10. Coles SJ, Easton P, Sharrod H, Hutson SM, Hancock J, Patel VB, Conway ME. S-Nitrosoglutathione inactivation of the mitochondrial and cytosolic BCAT proteins: S-nitrosation and S-thiolation. Biochemistry.;48(3):645-56, 2009.
11. Coles SJ, Hancock JT, Conway ME. Differential redox potential between the human cytosolic and mitochondrial branched-chain aminotransferase. Acta Biochim Biophys Sin (Shanghai).;44(2):172-6, 2012.
12. Conway ME, Coles SJ, Islam MM, et al. Regulatory control of human cytosolic branched-chain aminotransferase by oxidation and S-glutathionylation and its interactions with redox sensitive neuronal proteins. Biochem;47(19), 5465-5479, 2008.
13. Conway ME, Hutson SM. BCAA Metabolism and NH(3) Homeostasis. Adv Neurobiol.;13:99-132, 2016.
14. Conway ME, Lee C. The redox switch that regulates molecular chaperones. Biomol Concepts.;6(4):269-84, 2015
15. Conway ME, Poole LB, Hutson SM. Roles for cysteine residues in the regulatory CXXC motif of human mitochondrial branched chain aminotransferase enzyme. Biochemistry. 43(23), 7356-7364, 2004.
16. Conway ME, Yennawar N, Wallin R, Poole LB, Hutson SM. Human mitochondrial branched chain aminotransferase: structural basis for substrate specificity and role of redox active cysteines. Biochim Biophys Acta. 1647(1-2):61-5, 2003.

17. Conway ME, Yennawar N, Wallin R, Poole LB, Hutson SM. Identification of a peroxide-sensitive redox switch at the CXXC motif in the human mitochondrial branched chain aminotransferase. Biochemistry.;41(29):9070-8, 2002.

18. Cruz-Orcutt N, Vacaflores A, Connolly SF, Bunnell SC, Houtman JC. Activated PLC-γ1 is catalytically induced at LAT but activated PLC-γ1 is localized at both LAT- and TCR-containing complexes. Cell Signal. 26(4):797-805, 2014.

19. Dempsey EC, Newton AC, Mochly-Rosen D, Fields AP, Reyland ME, Insel PA, Messing RO. Protein kinase C isozymes and the regulation of diverse cell responses. Am J Physiol Lung Cell Mol Physiol. 279(3):L429-38, 2000.

20. Duncan, J.A.; Gilman, A.G. Characterization of Saccharomyces cerevisiae Acyl-protein Thioesterase 1, the Enzyme Responsible for G Protein α Subunit Deacylation in Vivo. J. Biol. Chem. 277, 31740–31752, 2002.

21. El Hindy M, Hezwani M, Corry D, Hull J, El Amraoui F, Harris M, Lee C, Forshaw T, Wilson A, Mansbridge A, Hassler M, Patel VB, Kehoe PG, Love S, Conway ME. The branched-chain aminotransferase proteins: novel redox chaperones for protein disulfide isomerase--implications in Alzheimer's disease. Antioxid Redox Signal.;20(16):2497-513, 2014.

22. El Hindy MEL, Conway ME. Redox-Regulated, Targeted Affinity Isolation of NADH-Dependent Protein Interactions with the Branched Chain Aminotransferase Proteins. Methods Mol Biol. 151-163, 2019.

23. Flores-Bellver M, Bonet-Ponce L, Barcia JM, Garcia-Verdugo JM, Martinez-Gil N, Saez-Atienzar S, Sancho-Pelluz J, Jordan J, Galindo MF, Romero FJ. Autophagy and mitochondrial alterations in human retinal pigment epithelial cells induced by ethanol: implications of 4-hydroxy-nonenal. Cell Death Dis. 5:e1328, 2014.

24. Gabuzda D, Busciglio J, Yankner BA. Inhibition of beta-amyloid production by activation of protein kinase C. J Neurochem. 61(6):2326-9, 1993.

25. García-Espinosa MA, Wallin R, Hutson SM, Sweatt AJ. Widespread neuronal expression of branched-chain aminotransferase in the CNS: implications for leucine/glutamate metabolism and for signaling by amino acids. J Neurochem. 100(6):1458-68, 2007.

26. Glick D, Barth S, Macleod KF. Autophagy: cellular and molecular mechanisms. J Pathol. 221(1):3-12, 2010.

27. Gopalakrishna R, Gundimeda U, Schiffman JE, McNeill TH. A direct redox regulation of protein kinase C isoenzymes mediates oxidant-induced neuritogenesis in PC12 cells. J Biol Chem. 283(21):14430-44, 2008.

28. Gopalakrishna R, Jaken S. Protein kinase C signaling and oxidative stress. Free Radic Biol Med. 28(9):1349-61, 2000.

29. Goto M, Miyahara I, Hirotsu K, Conway M, Yennawar N, Islam MM, Hutson SM. Structural determinants for branched-chain aminotransferase isozyme-specific inhibition by the anticonvulsant drug gabapentin. J Biol Chem. 280(44):37246-56, 2005.

30. Heras-Sandoval D, Pérez-Rojas JM, Hernández-Damián J, Pedraza-Chaverri J. The role of PI3K/AKT/mTOR pathway in the modulation of autophagy and the clearance of protein aggregates in neurodegeneration. Cell Signal. 26(12):2694-701, 2014.

31. Houtman JC, Higashimoto Y, Dimasi N, Cho S, Yamaguchi H, Bowden B, Regan C, Malchiodi EL, Mariuzza R, Schuck P, Appella E, Samelson LE. Binding specificity of multiprotein signaling complexes is determined by both cooperative interactions and affinity preferences. Biochemistry. 43(14):4170-8, 2004.
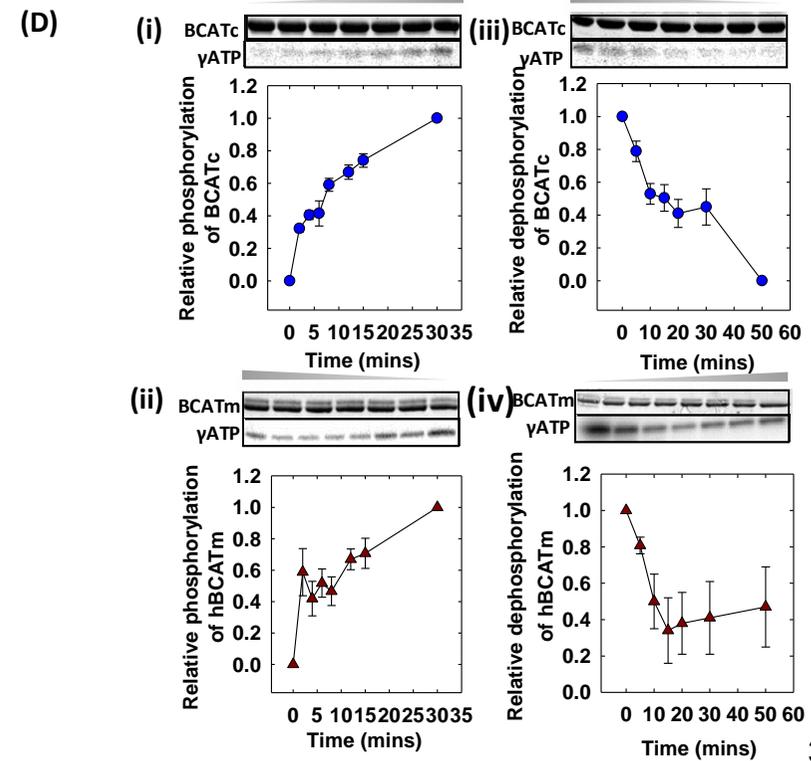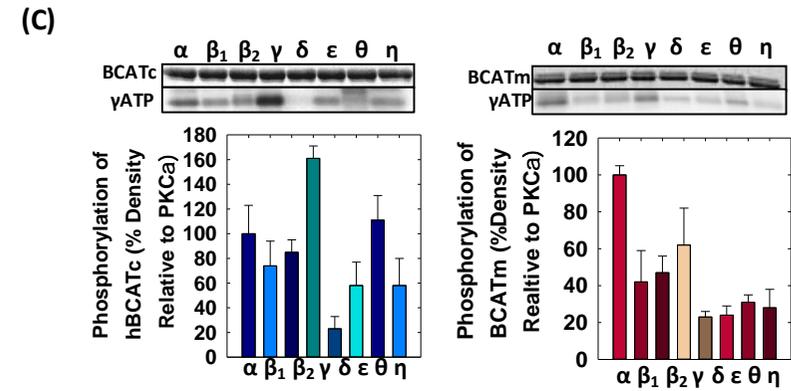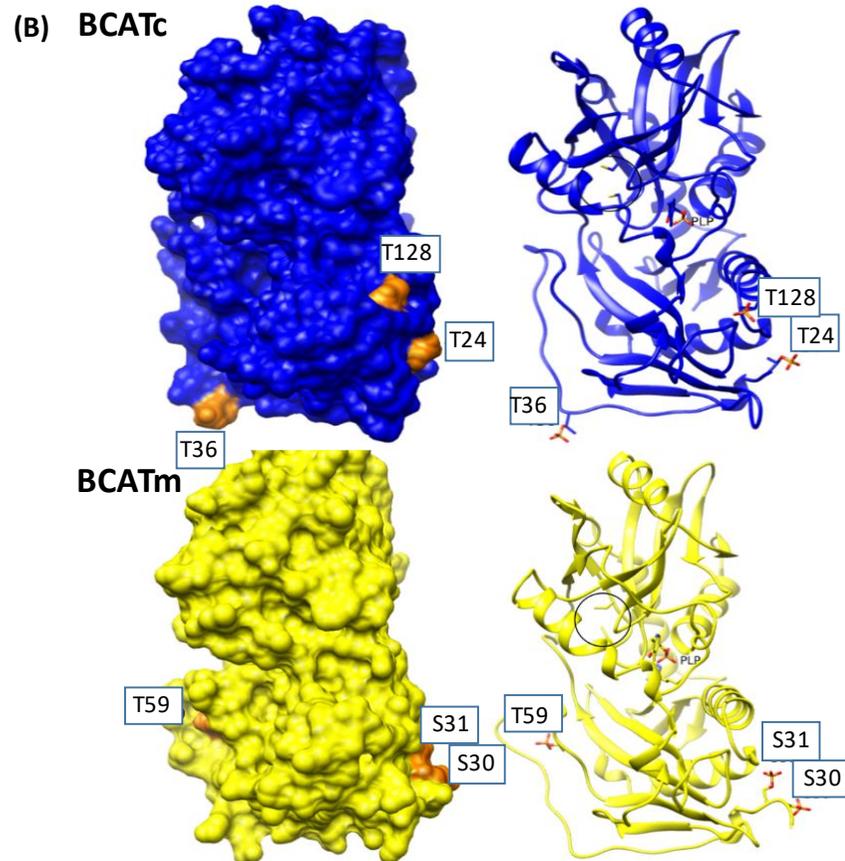
32. Huang R, Xu Y, Wan W, Shou X, Qian J, You Z, Liu B, Chang C, Zhou T, Lippincott-Schwartz J, Liu W. Deacetylation of nuclear LC3 drives autophagy initiation under starvation. Mol Cell. 57(3):456-66, 2015.

33. Hudd F, Shiel A, Harris M, Bowdler P, McCann B, Tsivos D, Wearn A, Knight M, Kauppinen R, Coulthard E, White P, Conway ME. Novel Blood Biomarkers that Correlate with Cognitive Performance and Hippocampal Volumetry: Potential for Early Diagnosis of Alzheimer's Disease. J Alzheimers Dis. 67(3):931-947, 2019.

34. Hull J, Hindy ME, Kehoe PG, Chalmers K, Love S, Conway ME. Distribution of the branched chain aminotransferase proteins in the human brain and their role in glutamate regulation. J Neurochem. 123(6):997-1009, 2012.

35. Hull J, Patel V, El Hindy M, Lee C, Odeleye E, Hezwani M, Love S, Kehoe P, Chalmers K, Conway M. Regional Increase in the Expression of the BCAT Proteins in Alzheimer's Disease Brain: Implications in Glutamate Toxicity. J Alzheimers Dis. 45(3):891-905, 2015.

36. Hung AY, Haass C, Nitsch RM, Qiu WQ, Citron M, Wurtman RJ, Growdon JH, Selkoe DJ. Activation of protein kinase C inhibits cellular production of the amyloid beta-protein. J Biol Chem. 268(31):22959-62, 1993.

37. Ichihara A. Isozyme patterns of branched-chain amino acid transaminase during cellular differentiation and carcinogenesis. Ann N Y Acad Sci. 259:347-54, 1975.

38. Islam MM, Nautiyal M, Wynn RM, et al. Branched-chain amino acid metabolon: interaction of glutamate dehydrogenase with the mitochondrial branched-chain aminotransferase (BCATm). J Biol Chem. 285(1):265-76, 2010.

39. Islam MM, Wallin R, Wynn RM, Conway M, Fujii H, Mobley JA, Chuang DT, Hutson SM. A novel branched-chain amino acid metabolon. Protein-protein interactions in a supramolecular complex. J Biol Chem. 282(16):11893-903, 2007.

40. Itakura E, Kishi C, Inoue K, Mizushima N. Beclin 1 forms two distinct phosphatidylinositol 3-kinase complexes with mammalian Atg14 and UVRAG. Mol Biol Cell. 19(12):5360-72, 2008.

41. Kim T, Hinton DJ, Choi DS. Protein kinase C-regulated aβ production and clearance. Int J Alzheimers Dis. 2011:857368, 2011.

42. Kong, E.; Peng, S.; Chandra, G.; Sarkar, C.; Zhang, Z.; Bagh, M.B.; Mukherjee, A.B. Dynamic palmitoylation links cytosol-membrane shuttling of acyl-protein thioesterase-1 and acyl-protein thioesterase-2 with that of proto-oncogene H-Ras product and growth associated protein-43. J. Biol. Chem. 288, 9112–9125, 2013.

43. Kurumatani T, Fastbom J, Bonkale WL, Bogdanovic N, Winblad B, Ohm TG, Cowburn RF. Loss of inositol 1,4,5-trisphosphate receptor sites and decreased PKC levels correlate with staging of Alzheimer's disease neurofibrillary pathology. BrainRes. 796(1-2):209-21, 1998.

44. Kuusisto E, Salminen A, Alafuzoff I. Ubiquitin-binding protein p62 is present in neuronal and glial inclusions in human tauopathies and synucleinopathies. Neuroreport. 12(10):2085-90, 2001.

45. LaNoue KF, Berkich DA, Conway M, Barber AJ, Hu LY, Taylor C, Hutson S. Role of specific aminotransferases in de novo glutamate synthesis and redox shuttling in the retina. J Neurosci Res. 66(5):914-22, 2001.

46. Lee W, Boo JH, Jung MW, Park SD, Kim YH, Kim SU, Mook-Jung I. Amyloid beta peptide directly inhibits PKC activation. Mol Cell Neurosci. 26(2):222-31, 2004.

47. Li J, Huang FL, Huang KP. Glutathiolation of proteins by glutathione disulphide S-oxide derived from S-nitrosoglutathione. Modifications of rat brain neurogranin/RC3 and neuromodulin/GAP-43. J Biol Chem. 276(5):3098-105, 2001.
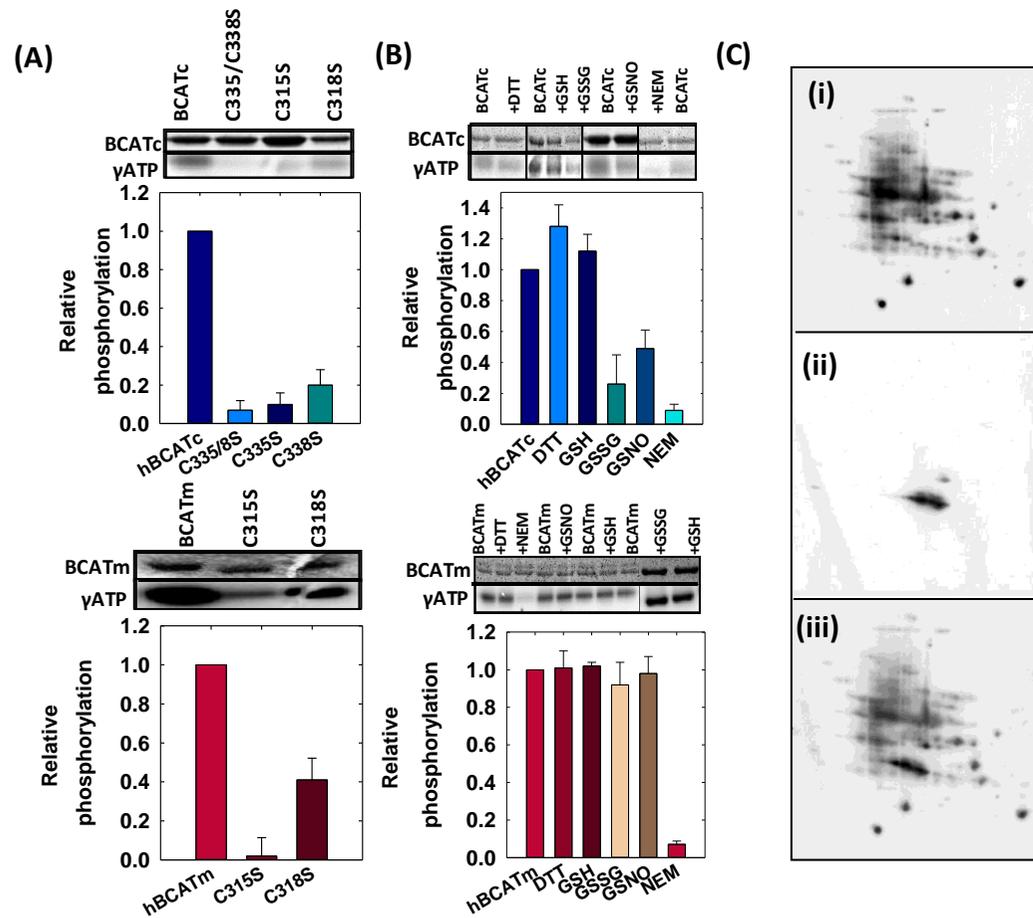
48. Lieth E, LaNoue KF, Berkich DA, et al. Nitrogen shuttling between neurons and glial cells during glutamate synthesis. J Neurochem. 76(6):1712-1723, 2001.

49. Linder, M.E.; Deschenes, R.J. Model organisms lead the way to protein palmitoyl transferases. J. Cell Sci. 117 Pt 4, 521–526, 2004.

50. Mauthe M, Orhon I, Rocchi C, Zhou X, Luhr M, Hijlkema KJ, Coppes RP, Engedal N, Mari M, Reggiori F. Chloroquine inhibits autophagic flux by decreasing autophagosome-lysosome fusion. Autophagy. 14(8):1435-1455, 2018.

51. Mauvezin C, Neufeld TP. Bafilomycin A1 disrupts autophagic flux by inhibiting both V-ATPase-dependent acidification and Ca-P60A/SERCA-dependent autophagosome-lysosome fusion. Autophagy. 11(8):1437-8, 2015.

52. Miao HH, Ye JS, Wong SL, Wang BX, Li XY, Sheu FS. Oxidative modification of neurogranin by nitric oxide: an amperometric study. Bioelectrochemistry. 51(2):163-73, 2000.

53. Moore P, White J, Christiansen V, Grammas P. Protein kinase C-zeta activity but not level is decreased in Alzheimer's disease microvessels. Neurosci Lett. 254(1):29-32, 1998.

54. Nakamura, T. and Lipton, S.A. Cell death: protein misfolding and neurodegenerative diseases. Apoptosis: An International Journal on Programmed Cell Death 14 (4), 455-468, 2009.

55. Nakaso K, Yoshimoto Y, Nakano T, Takeshima T, Fukuhara Y, Yasui K, Araga S, Yanagawa T, Ishii T, Nakashima K. Transcriptional activation of p62/A170/ZIP during the formation of the aggregates: possible mechanisms and the role in Lewy body formation in Parkinson's disease. Brain Res. 1012(1-2):42-51, 2004.

56. Nixon, R.A. Autophagy, amyloidogenesis and Alzheimer disease. J Cell Sci.;120 (Pt 23):4081-91, 2007.

57. Nixon RA, Wegiel J, Kumar A, Yu WH, Peterhoff C, Cataldo A, Cuervo AM.Extensive involvement of autophagy in Alzheimer disease: an immuno-electron microscopy study. J Neuropathol Exp Neurol. 64(2):113-22, 2005.

58. Perez SE, He B, Nadeem M, Wuu J, Ginsberg SD, Ikonomovic MD, Mufson EJ. Hippocampal endosomal, lysosomal, and autophagic dysregulation in mild cognitive impairment: correlation with aβ and tau pathology. J Neuropathol Exp Neurol. 74(4):345-58, 2015.

59. Pessin JE, Saltiel AR. Signaling pathways in insulin action: molecular targets of insulin resistance. J Clin Invest. 106(2):165-9. 2000.

60. Saito N, Shirai Y. Protein kinase C gamma (PKC gamma): function of neuron specific isotype. J Biochem. 132(5):683-7, 2002.

61. Shafei MA, Harris M, Conway ME. Divergent Metabolic Regulation of Autophagy and mTORC1-Early Events in Alzheimer's Disease? Front Aging Neurosci. 2;9:173, 2017.

62. Sheu FS, Mahoney CW, Seki K, Huang KP. Nitric oxide modification of rat brain neurogranin affects its phosphorylation by protein kinase C and affinity for calmodulin. J Biol Chem. 271(37):22407-13, 1996.

63. Shin, H.J., Kim, H., Oh, S., Lee, J.-G., Kee, M., Ko, H.-J., Kweon, M.-N., Won, K.J., and Baek, S.H.. AMPK-SKP2-CARM1 signalling cascade in transcriptional regulation of autophagy. Nature 534, 553–557, 2016.

64. Sontag JM, Sontag E. Protein phosphatase 2A dysfunction in Alzheimer's disease. Front Mol Neurosci. 11;7:16, 2014.
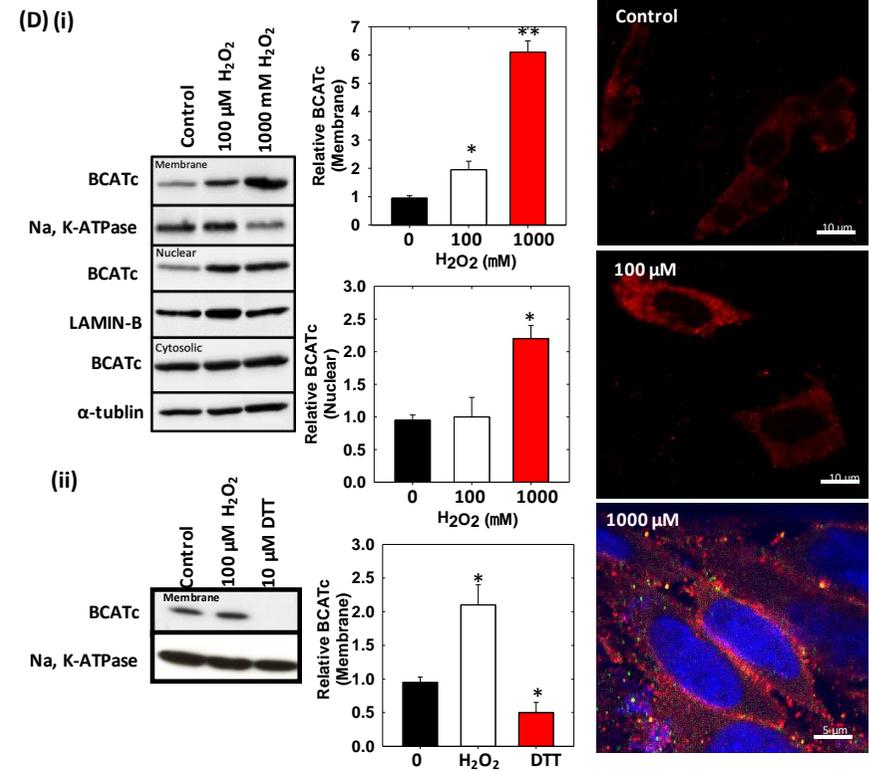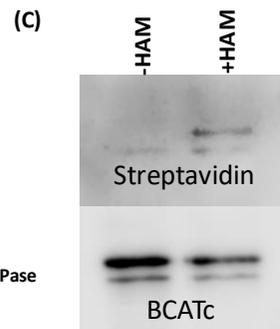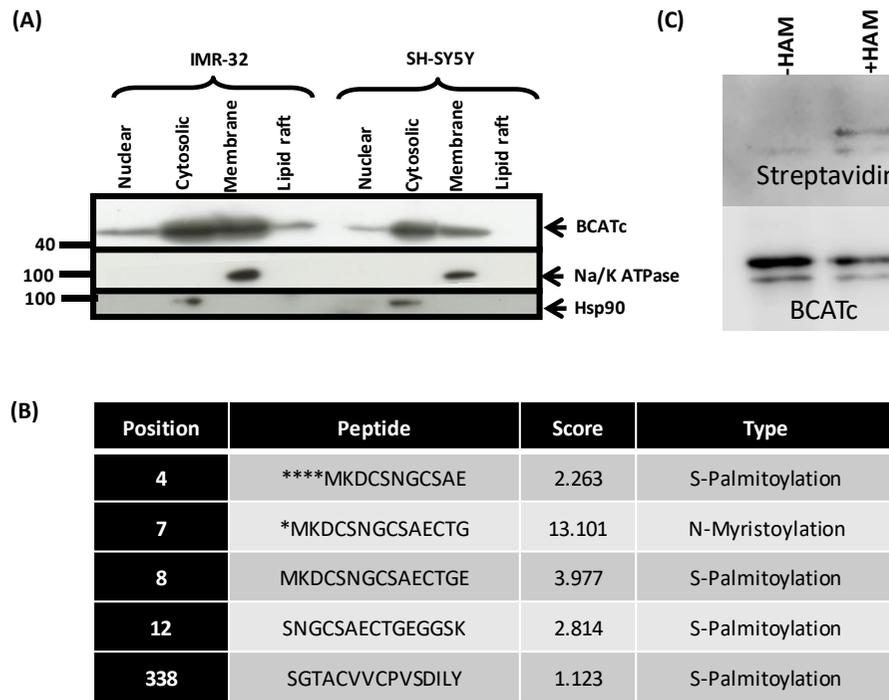
65. Spinelli M, Fusco S, Grassi C. Nutrient-Dependent Changes of Protein Palmitoylation: Impact on Nuclear Enzymes and Regulation of Gene Expression. Int J Mol Sci. 19(12). pii: E3820, 2018.
66. Steinberg SF. Structural basis of protein kinase C isoform function. PhysiolRev.;88(4):1341-78, 2008.
67. Steinberg SF. Mechanisms for redox-regulation of protein kinase C. Front Pharmacol.;6:128, 2015.
68. Wei, X.; Song, H.; Semenkovich, C.F. Insulin-Regulated Protein Palmitoylation Impacts Endothelial Cell Function. Arterioscler. Thromb. Vasc. Biol. 34, 346–354, 2014.
69. Yennawar NH, Conway ME, Yennawar HP, Farber GK, Hutson SM. Crystal structures of human mitochondrial branched chain aminotransferase reaction intermediates: ketimine and pyridoxamine phosphate forms. Biochemistry.;41(39):11592-601, 2002.
70. Yennawar NH, Islam MM, Conway M, Wallin R, Hutson SM. Human mitochondrial branched chain aminotransferase isozyme: structural role of the CXXC center in catalysis. J Biol Chem. 281(51):39660-71, 2006.
71. Yu WH, Cuervo AM, Kumar A, Peterhoff CM, Schmidt SD, Lee JH, Mohan PS, Mercken M, Farmery MR, Tjernberg LO, Jiang Y, Duff K, Uchiyama Y, Näslund J, Mathews PM, Cataldo AM, Nixon RA. Macroautophagy--a novel Beta-amyloid peptide-generating pathway activated in Alzheimer's disease. J Cell Biol. 171(1):87-98, 2005.
72. Yu WH, Kumar A, Peterhoff C, Shapiro Kulnane L, Uchiyama Y, Lamb BT, Cuervo AM, Nixon RA. Autophagic vacuoles are enriched in amyloid precursor protein-secretase activities: implications for beta-amyloid peptide over-production and localization in Alzheimer's disease. Int J Biochem Cell Biol. 36(12):2531-40, 2004.
73. Zhang Y, Wu Y, Tashiro S, Onodera S, Ikejima T. Involvement of PKC signal pathways in oridonin-induced autophagy in HeLa cells: a protective mechanism against apoptosis. Biochem Biophys Res Commun. 378(2):273-8, 2009.
74. Zhou YY, Li Y, Jiang WQ, Zhou LF. MAPK/JNK signalling: a potential autophagy regulation pathway. Biosci Rep. 35(3), 2015.
75. Zhu G, Wang D, Lin YH, McMahon T, Koo EH, Messing RO. Protein kinase C epsilon suppresses Abeta production and promotes activation of alpha-secretase. Biochem Biophys Res Commun. 285(4):997-1006, 2001.
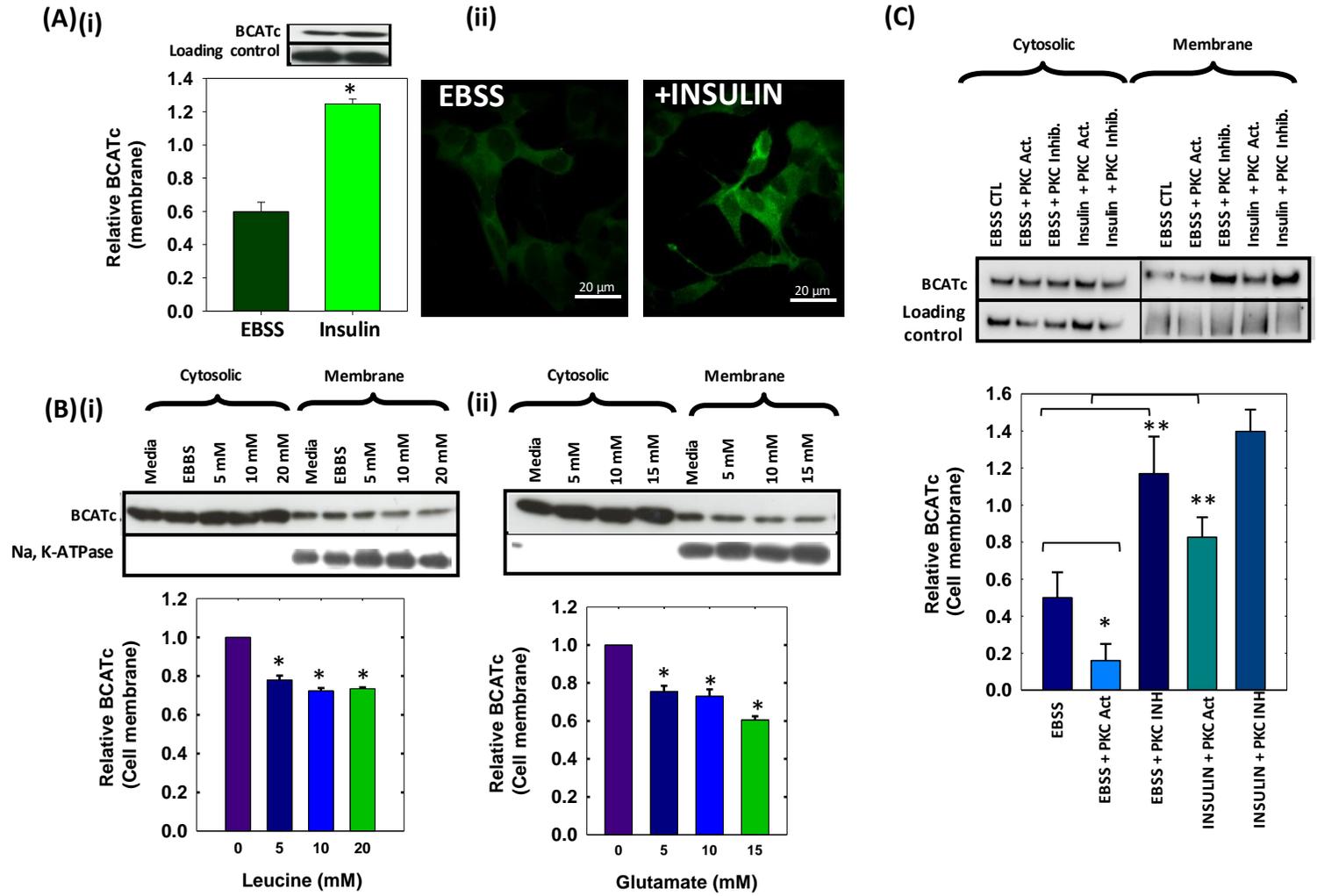
(A)

BCATc				
PKC α, β, γ, δ, ε				
Site	Score	Percentile	Sequence	SA
T24	0.519	3.33	GSKEVVGTFKAKDLI	0.4
T36	0.510	3.00	DLIVTPATILKEKPD	0.6
T128	0.496	2.31	YRSAVRATLPVFDKEMLM	0.6
BCATm				
PKC α, β, γ, δ, ε				
Site	Score	Percentile	Sequence	SA
S30	0.519	3.519	GPRRYASS SFKAADL	0.96
S31	0.509	2.933	PRRYASS SFKAADLQ	0.96
T59	0.531	4.906	EPLVFGKTH TDHMLM	2.14

(B)

BCATc

BCATm

(C)

(D)

31

(A)

IMR-32 | SH-SY5Y

Nuclear | Cytosolic | Membrane | Lipid raft | Nuclear | Cytosolic | Membrane | Lipid raft

← BCATc
40
100 ← Na/K ATPase
100 ← Hsp90

(C)

-HAM | +HAM

Streptavidin

BCATc

(B)

Position	Peptide	Score	Type
4	****MKDCSNGCSAE	2.263	S-Palmitoylation
7	*MKDCSNGCSAECTG	13.101	N-Myristoylation
8	MKDCSNGCSAECTGE	3.977	S-Palmitoylation
12	SNGCSAECTGEGGSK	2.814	S-Palmitoylation
338	SGTACVVCPVSDILY	1.123	S-Palmitoylation

(D) (i)

Control | 100 μM H_2O_2 | 1000 mM H_2O_2

BCATc — Membrane
Na, K-ATPase
BCATc — Nuclear
LAMIN-B
BCATc — Cytosolic
α-tublin

Relative BCATc (Membrane) vs H_2O_2 (mM): 0, 100 *, 1000 **

Relative BCATc (Nuclear) vs H_2O_2 (mM): 0, 100, 1000 *

(ii)

Control | 100 μM H_2O_2 | 10 μM DTT

BCATc — Membrane
Na, K-ATPase

Relative BCATc (Membrane): 0, H_2O_2 *, DTT *

Control
10 μm

100 μM
10 μm

1000 μM
5 μm

(A)(i)

BCATc
Loading control

(ii)

EBSS +INSULIN

20 µm   20 µm

(C)

Cytosolic   Membrane

EBSS CTL
EBSS + PKC Act.
EBSS + PKC Inhib.
Insulin + PKC Act.
Insulin + PKC Inhib.

BCATc
Loading control

(B)(i)   **(ii)**

Cytosolic   Membrane   Cytosolic   Membrane

BCATc
Na, K-ATPase

Leucine (mM)   Glutamate (mM)